Pressure effects on magnetic and transport properties of electron-doped $La_{1-x}Ca_xMnO_3$ ($x=0.8, 0.9$)

V. Markovich,[1,*] I. Fita,[2,3] R. Puzniak,[2] E. Rozenberg,[1] C. Martin,[4] A. Wisniewski,[2] Y. Yuzhelevski,[1] and G. Gorodetsky[1]

[1]*Department of Physics, Ben-Gurion University of the Negev, P.O. Box 653, 84105 Beer-Sheva, Israel*

[2]*Institute of Physics, Polish Academy of Sciences, Aleja Lotnikow 32/46, PL-02-668 Warsaw, Poland*

[3]*Donetsk Institute for Physics and Technology, NAS, R. Luxemburg str. 72, 83114 Donetsk, Ukraine*

[4]*Laboratoire CRISMAT, UMR 6508, ISMRA, 6 Boulevard du marechal Juin, 14050 Caen Cedex, France*

(Received 15 August 2004; revised manuscript received 16 November 2004; published 29 April 2005)

Magnetic and transport properties of polycrystalline $La_{1-x}Ca_xMnO_3$ ($x=0.8, 0.9$) perovskites were investigated in the temperature range 4.2–300 K, magnetic field up to 16 kOe and under hydrostatic pressures up to 12 kbar. The $La_{0.1}Ca_{0.9}MnO_3$ compound exhibits a heterogeneous spin configuration in its ground state [*G*-type antiferromagnetic (AFM) phase with local ferromagnetic (FM) regions and *C*-type AFM]. The $x=0.8$ compound is mostly an orbital ordered *C*-type AFM. In the case of $La_{0.1}Ca_{0.9}MnO_3$, an applied pressure slightly increases the magnetic transition temperature and significantly enhances the FM component. Pronounced hysteretic effects observed in $La_{0.1}Ca_{0.9}MnO_3$ may be attributed to the competition between the FM and AFM fractions in the *G*-AFM structure. On the other hand, $La_{0.2}Ca_{0.8}MnO_3$ is insensitive to applied pressure probably due to a robustness of orbital ordered state. Resistivity data point out that AFM ordering in $La_{0.2}Ca_{0.8}MnO_3$ occurs at temperatures below orbital ordering.

DOI: 10.1103/PhysRevB.71.134427 PACS number(s): 75.30.Kz, 71.30.+h, 74.62.Fj

Perovskite manganites $La_{1-x}Ca_xMnO_3$ have been extensively investigated after the discovery of colossal magnetoresistance effect in optimally doped $x\sim0.33$ composition.[1,2] It is widely accepted that the basic mechanism for electron transport in these oxides is a double exchange (DE) interaction mediated by hopping of spin-polarized e_g electrons, between Mn^{3+} and Mn^{4+}, thereby facilitating metallic electrical conductivity and ferromagnetism. It is well accepted[1] that the DE is also accounted for by electronic phase separation (PS) and the formation of ferromagnetic metallic (FMM) clusters in an antiferromagnetic (AFM) matrix. In general, the FMM phase occurs in hole-doped regime: $0.22<x<0.5$. For $x>0.5$ the electron-doped manganites are dominated by charge ordering (CO) and do not show a FM ground state at all. The complexity of manganites stems from the interplay between several competing interactions of comparable intensity. Particularly, the electron-phonon coupling, associated with Jahn-Teller (JT) distortions of the MnO_6 octahedra plays an important role in the insulator to metal transition. The distortions of the octahedra may give rise to the localization of the e_g electrons.

$CaMnO_3$, the end compound of $(La,Ca)MnO_3$ system, is a *G*-type antiferromagnet[3] ($T_N\sim120$ K) in its ground state possessing a weak FM component.[2,4] In the above spin configuration, each Mn magnetic moment is antiparallel to its nearest Mn neighbors. Based on measurements of the resistivity and magnetization, Neumeier and Cohn[5] have distinguished four regions in the compositional range $0.8<x<1$. Region I ($0.98<x<1.0$) contains a *G*-type AFM and local ferrimagnetism. Region II ($0.93<x<0.98$) contains local FM regions in a *G*-type AFM matrix. Region III ($0.84<x<0.93$) contains *G*-type AFM, *C*-type AFM, and local FM regions. Region IV ($0.80<x<0.84$) is a *C*-type AFM. It should be emphasized that the significant enhancement of the spontaneous magnetization around $x\approx0.9$, is a common feature of $Ln_{1-x}Ca_xMnO_3$ [Ln=Pr,[6,7] Nd,[8] Gd,[8] Y,[8] Sm (see Refs. 7,9)] manganites. For $x=0.8$ (depending on Ln) the CO dominates and the spontaneous magnetization is close to zero.[5,6,7,9] Refined neutron diffraction (ND) data[10–13] of $La_{1-x}Ca_xMnO_3$ ($0.5<x<1$) have shown the evolution of magnetic and crystallographic phases with doping and temperature.

It should be noted that the effect of pressure (P) on magnetic and transport properties of hole-doped $La_{1-x}Ca_xMnO_3$ (LCMO) samples was the subject of a number of investigations.[14–18] However, investigation of the effect of pressure on magnetic and transport properties of $Ln_{1-x}Ca_xMnO_3$ (Ln=rare earth) manganites in low-electron-doped regime ($0.8\leqslant x\leqslant1$) is quite scarce. There are only studies of charge ordered $Sm_{0.2}Ca_{0.8}MnO_3$ (see Ref. 19) and mixed $Y_{1-x}Ca_xMnO_3$ and $Sm_{1-x}Ca_xMnO_3$ ($0.85\leqslant x\leqslant0.95$) with competing FM and AFM phases.[20] It should be noted that the phase diagrams of $Ln_{1-x}Ca_xMnO_3$ exhibit a kind of asymmetry with regard to magnetic properties around the $x=0.5$. For example, in the region of electron doping ($x>0.5$) ferromagnetic ground state was not observed, whereas in the hole-doping region ($x<0.5$) FM state prevails in the most of this region. This asymmetry may be accounted for by the strong JT distortions in the hole-doped regime with a high enough amount of JT active Mn^{3+} ions, while in the electron-doped regime with the most JT nonactive Mn^{4+} ions, the JT effects are not expected to contribute to transport properties and magnetic ordering in the same way they are expected for hole doping. Nevertheless, recently, ND data have revealed static JT distortion in $La_{1-x}Ca_xMnO_3$ ($x=0.8, 0.85$) with low content of Mn^{3+}.[10] For the study of the pressure effect on magnetic and transport properties of electron-doped manganites, we have chosen two compounds $La_{1-x}Ca_xMnO_3$ ($x=0.8, 0.9$) that show distinct magnetic and transport properties at ambient pressure and have been ex-

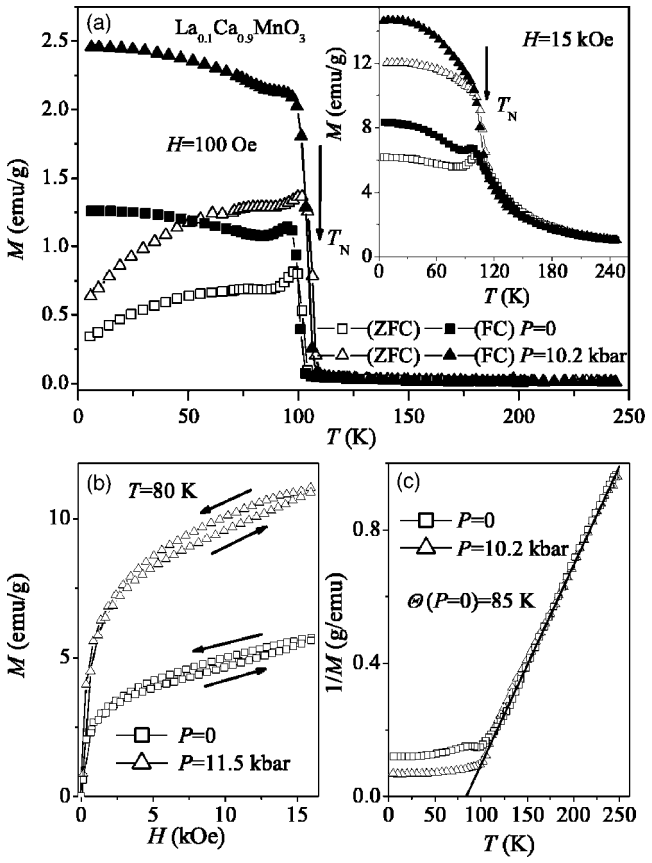

FIG. 1. (a) Temperature dependence of M_{ZFC} and M_{FC} magnetization for $La_{0.1}Ca_{0.9}MnO_3$ at $P=0$ and $P=10.2$ kbar in magnetic field $H=100$ Oe. Inset shows M_{ZFC} and M_{FC} at $P=0$ and $P=10.2$ kbar in magnetic field $H=15$ kOe. (b) Field dependence of magnetization at 80 K under $P=0$ and $P=11.5$ kbar. (c) $1/M$ vs temperature curves for $La_{0.1}Ca_{0.9}MnO_3$ at $P=0$ and $P=10.2$ kbar. Solid line is a guide to the eye.

tensively studied recently by ND measurements.[10–13] Measurements performed under pressure allowed us to find which interactions play a dominant role in a given system, i.e., we were able to distinguish if the dominant is competing AFM-FM or orbital ordering.

Measurements were carried out on polycrystalline samples, prepared by a standard ceramic route in air at 1450 °C, starting from stoichiometric ratios of CaO, La_2O_3, and MnO_2, with intermediate crushing and heating. The x-ray data at room temperature were found to be compatible with an orthorhombic unit cell of *Pnma* space group of a perovskite structure with the lattice parameters: $a=5.3343$ Å, $b=7.5519$ Å, $c=5.3288$ Å, and $a=5.3104$ Å, $b=7.4970$ Å, $c=5.3005$ Å for $x=0.8$ and $x=0.9$ samples, respectively. Powder x-ray diffraction revealed no secondary phases. The experimental procedures of the magnetic and transport measurements under high hydrostatic pressure are described in detail elsewhere.[18,19]

Figure 1(a) shows the results obtained for zero field cooled (M_{ZFC}) and field cooled (M_{FC}) magnetization of $La_{0.1}Ca_{0.9}MnO_3$ vs temperature under ambient pressure ($P=0$) and $P=10.2$ kbar in magnetic field $H=100$ Oe. It appears that the magnetization sharply rises on cooling at about

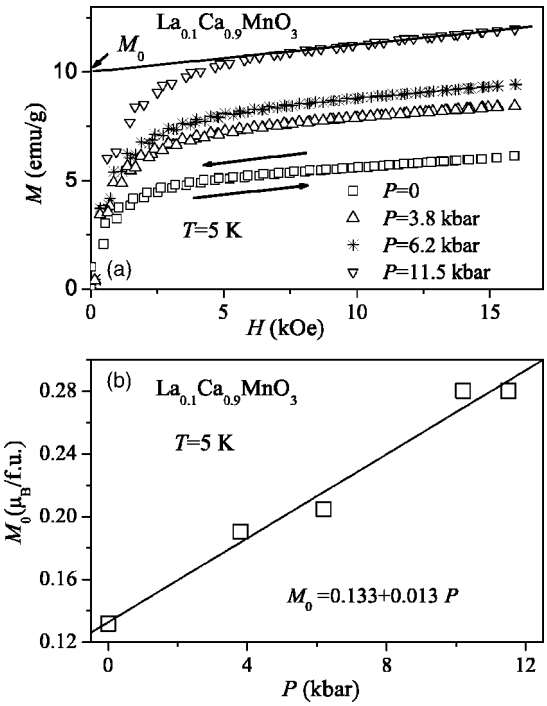

FIG. 2. (a) Field dependence of magnetization at 5 K under various pressures. (b) A variation of M_0 for $La_{0.1}Ca_{0.9}MnO_3$ at $T=5$ K with pressure.

107 K, a critical temperature that coincides with the Néel temperature.[10–13] Note that $M(T)$ displays a minimum around $T\approx 85$ K, at ambient pressure in magnetic field of 15 kOe, which disappears at $P=10.2$ kbar [inset to Fig. 1(a)]. $M(H)$ shows some hysteretic effects in this temperature region [see Fig. 1(b)]. The plot of $1/M$ vs T of FC curves at 15 kOe [inset of Fig. 1(a)] is given in Fig. 1(c). It appears that above the transition temperature the curves obey the relation $1/M=C/(T-\Theta)$, where Θ changes from -350 K for parent $CaMnO_3$ (see Refs. 21,22) to 85 K for $La_{0.1}Ca_{0.9}MnO_3$. This means that the dominant effective magnetic interactions change from AFM to FM ones upon doping of Ca by 10% of La, and they practically do not depend on applied pressure.

Figure 2(a) shows the magnetization of $La_{0.1}Ca_{0.9}MnO_3$ vs magnetic fields at 5 K, under various pressures. The weak spontaneous magnetization M_0 shown in Fig. 2(a) is attributed to the FM phase, whereas the AFM phase gives rise to the linear $M(H)$ dependence in the high-field region. The coercive field H_C is ≈ 0 for all of the applied pressures at 5 and 80 K [see Figs. 1(b) and 2(a)]. Interestingly, the spontaneous weak magnetization ($M_0=0.13$ μ_B/f.u. at $P=0$) obtained by a linear extrapolation of the high-field magnetization to $H=0$, is found to be strongly pressure dependent. M_0 increases linearly with increasing pressure and approaches a value of $M_0=0.28$ μ_B/f.u. at $P\sim 11$ kbar [see Fig. 2(b)].

Figure 3(a) presents the temperature dependence of the resistivity of $La_{0.1}Ca_{0.9}MnO_3$ at $P=0$ and $P=9.1$ kbar. Both curves exhibit a metallic behavior ($d\rho/dT>0$) at temperatures 225–300 K and the resistivity then increases with decreasing temperature. The quasi-metallic behavior of $La_{0.1}Ca_{0.9}MnO_3$ at $T>200$ K was observed previously by Neumeier and Cohn.[5] They pointed out that the temperature

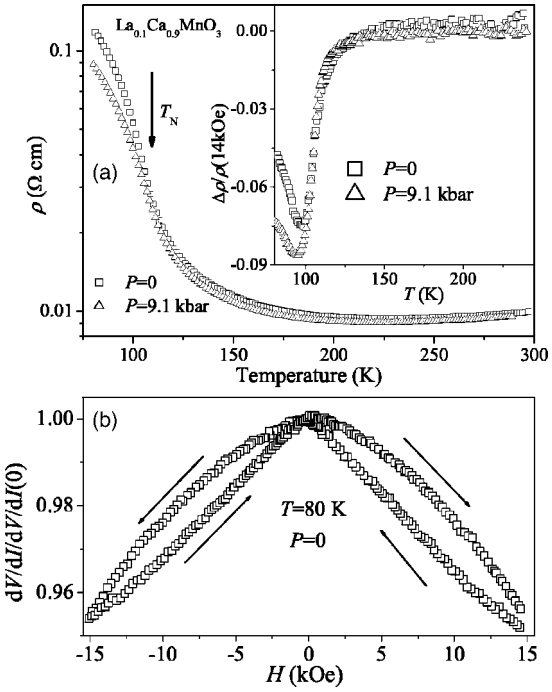

FIG. 3. (a) Temperature dependence of resistivity for $La_{0.1}Ca_{0.9}MnO_3$ at $P=0$ and $P=9.1$ kbar. Inset shows the temperature dependence of magnetoresistance at $P=0$ and $P=9.1$ kbar, where $\Delta\rho=\rho(14\ \text{kOe})-\rho(0)$. (b) Normalized hysteresis loops of dynamic resistivity for $La_{0.1}Ca_{0.9}MnO_3$ at $T=80$ K under $P=0$.

dependence of $\rho(T)$ observed is typical for heavily doped, *n*-type semiconductors, and positive temperature coefficient observed at $T>200$ K indicates that the chemical potential is positioned in the conduction band.[5] The effect of applied pressure on the resistivity is definitely seen only below T_N (that is also a T_C). The inset in Fig. 3(a) displays the variation of the magnetoresistance (MR) with temperature, showing the following features: (i) The resistivity practically does not depend on magnetic fields in temperature region 130–300 K, while a relatively modest MR is seen in the vicinity of T_N. (ii) MR maximizes at temperatures slightly below T_N [Fig. 1(a)], namely, the maximum of MR is observed at temperatures of 98 and 95 K for $P=0$ and $P=9.1$ kbar, respectively. Figure 3(b) shows the hysteresis loop of normalized dynamical resistivity $R_d=dV/dI(H)/dV/dI(0)$ recorded after zero field cooling to 80 K.

Figure 4 shows magnetization curves vs temperature for $La_{0.2}Ca_{0.8}MnO_3$. After the sample was cooled in zero magnetic field, the magnetization was measured upon heating and immediately thereafter upon cooling under a magnetic field $H=15$ kOe. Peaks around 214 K at cooling and around 220 K at heating ($P=0$) occur near the structural phase transition at temperature of orbital ordering, T_{OO}.[10–13] A significant hysteresis of about 10 K is observed at $P=0$. It was found that an applied pressure produces a suppression of magnetization in the vicinity of T_{OO} and also at $T>T_{OO}$. Under a pressure of 11.2 kbar, the magnetization peaks occur at 210 and 213 K for cooling and heating, respectively (Fig. 4), i.e., the hysteresis is also decreased under pressure. Contrary to the case of $La_{0.1}Ca_{0.9}MnO_3$, the $M(H)$ curves of $La_{0.2}Ca_{0.8}MnO_3$ do not display spontaneous magnetization below T_{OO} (see inset in Fig. 4), in agreement with results previously reported.[10]

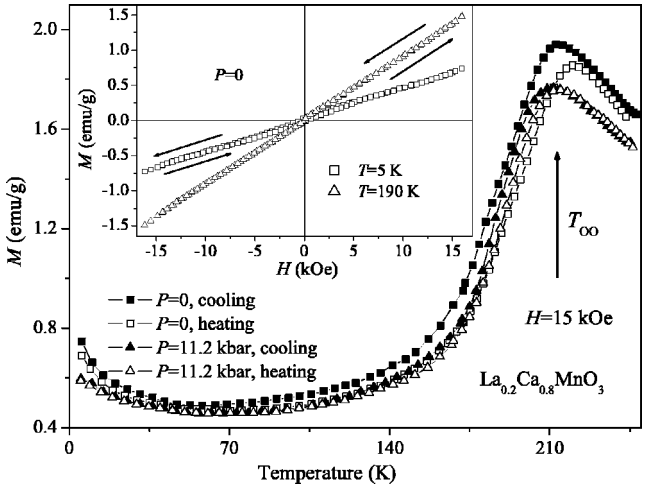

FIG. 4. Temperature dependence of magnetization after zero field cooling for $La_{0.2}Ca_{0.8}MnO_3$ at $P=0$ and $P=11.2$ kbar in magnetic field $H=15$ kOe. Inset shows hysteresis loops for ambient pressure at $T=5$ and 190 K.

Figure 5 presents the temperature dependence of the resistivity of $La_{0.2}Ca_{0.8}MnO_3$ for $P=0$ and $P=10.2$ kbar. It appears that an applied pressure slightly reduces the resistivity $La_{0.2}Ca_{0.8}MnO_3$ at temperatures 80–300 K. A maximal decrease in the resistivity, of about 20%, is observed at $T=80$ K. The $\rho(T)$ curves for both $P=0$ and $P=10.2$ kbar exhibit some anomalies in the range 170–190 K, as can be seen from the semilogarithmic dependence (Fig. 5). It was found previously[5] that the resistivity of $La_{1-x}Ca_xMnO_3$ ($0.8\leqslant x\leqslant 1$) at temperatures 50 K$\leqslant T\leqslant$150 K can be described by a single activation energy E_a, i.e., $\rho(T)=\rho_0\exp(E_a/k_BT)$, for which $E_a\approx 85$ meV for $x=1$, $E_a\approx 30$ meV for

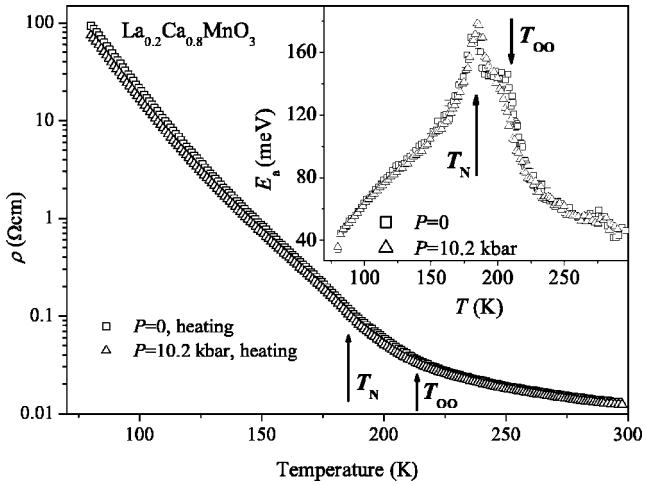

FIG. 5. Temperature dependence of resistivity for $La_{0.2}Ca_{0.8}MnO_3$ at $P=0$ and $P=10.2$ kbar. Inset shows the activation energy determined numerically by calculating $d\ln(\rho)/d(k_BT)^{-1}$ from resistivity data for $P=0$ and $P=10.2$ kbar.

$0.9 \leqslant x \leqslant 0.995$, and $E_a \approx 85-95$ meV for $0.8 \leqslant x \leqslant 0.88$. Activation energy E_a, in our case determined numerically by calculating $d\ln(\rho)/d(k_BT)^{-1}$ from resistivity data and shown in the inset of Fig. 5, is different than that given in Ref. 5. Apparently, the change in E_a at ~210 K (see Fig. 5) corresponds to the orbital ordering (OO). E_a peaks at $T_N \approx 185$ K, and decreases with decreasing temperature, a characteristic feature of magnetic semiconductors, where E_a depends strongly on the long-range magnetic order.[23] A similar behavior of $E_a(T)$ was observed recently for $Pr_{0.65}Ca_{0.35}MnO_3$ by Cui and Tyson.[24] They used the E_a peak as a mark for the shift in T_{CO} with pressure, but noted that the charge ordering occurs at higher temperatures.

Numerous investigations of magnetic and crystallographic PS in low-electron-doped $Ln_{1-x}Ca_xMnO_3$ $(0.8 \leqslant x \leqslant 1)$[1,2,6,13] have shown that a mixture of *G*- and *C*-type AFM phases associated with *Pnma* and $P2_1/m$ crystalline structures, respectively, is a distinctive feature of these materials. Analogously, for the $La_{1-x}Ca_xMnO_3$ case, high-resolution ND data[10–13] suggest that mesoscopic phases, of *C*-AFM regions (with no FM moment) and regions with coupled *G*-AFM +FM moments coexist. The evolution of the monoclinic phase fraction at 20 K with La substitution has shown that the above spin and crystallographic structures start to develop in $CaMnO_3$ with 6% La doping, and the ratio (monoclinic/orthorhombic) reaches about 20% and about 85% for $x=0.9$ and $x=0.8$, respectively.[12,13] Temperature variation of lattice parameters for $La_{0.1}Ca_{0.9}MnO_3$ has shown that magnetic ordering to *G*- and *C*-type AFM-magnetic structures occur concurrently with structural phase transition, when the *b* axis decreases, the *a* axis increases, and the *c* axis remains nearly constant.[11] According to Granado *et al.*,[13] *G*-type AFM matrix of $La_{1-x}Ca_xMnO_3$ $(0.85 < x < 0.95)$ allows two types of FM contributions: (i) relatively small FM droplets having the average size of ~10 Å, the concentration of which in the *G*-AFM matrix is proportional to La doping; and (ii) the long-range FM component perpendicularly coupled to *G*-AFM moments.

As already noted, the temperature and magnetic field dependences of the magnetization and resistivity for $La_{0.1}Ca_{0.9}MnO_3$ (Figs. 1–3) show remarkable features: (i) a large difference between both M_{ZFC} and M_{FC} curves, enhanced by applied pressure; and (ii) both $\rho(H)$ and $M(H)$ exhibit a hysteretic effect. Generally, the difference between M_{FC} and M_{ZFC} in manganites is induced by a "freezing" of magnetic moments in directions energetically favored by their local anisotropy or by external field and due to FM-cluster glass behavior.[1,2] In the case of $La_{0.1}Ca_{0.9}MnO_3$, such effects may be enhanced by strong competition between different magnetic and crystallographic structures, because $x=0.9$ sample exhibits not only a structural phase transition followed by two magnetic transitions T_N(*C*-AFM) and T_N(*G*-AFM), but also a clear decrease in the *C*-AFM order parameter below T_N(*G*-AFM).[12] Similar effects were observed recently for $Pr_{0.125}Ca_{0.875}MnO_3$.[6] Fujishiro *et al.*[6] suggested that magnetic-field-induced lattice transformation between two different crystallographic phases is also a source of hysteretic effects. Algarabel *et al.*[25] have shown using high-resolution ND, that the application of magnetic field in $Sm_{0.15}Ca_{0.85}MnO_3$ affects the ratio between *C*-AFM-$P2_1/m$ and *G*-AFM+FM-*Pnma* phases, favoring certainly *G*-AFM +FM-*Pnma* phase at the expense of *C*-AFM-$P2_1/m$ one. This effect was found to be relatively small at low temperatures ($T \ll T_N$), and increases with increasing temperature ($T < T_N$), where competing phases are very close in energy.[25] At a temperature of 100 K, an applied magnetic field changes the ratio of phases fractions from 10/90% for (*G* -AFM+FM-*Pnma*)/(*C*-AFM-$P2_1/m$) at $H=0$, to ~60/40% under an applied field of 60 kOe. The application of magnetic fields at 5 K in the case of $La_{0.09}Ca_{0.91}MnO_3$ have markedly changed the intensity of both *G*-AFM and *G*-FM magnetic Bragg peaks even at a magnetic field of 5 kOe, while for *C*-AFM phase, the reflections are insensitive to the field up to 70 kOe.[13] One may conclude from the above observations that at low temperatures, where both *C*-AFM -$P2_1/m$ and *G*-AFM+FM-*Pnma* phases differ in their energy, the application of a magnetic field results only in a reorientation of the FM spin component (associated with *G* -AFM+FM-*Pnma* phase) along the field direction and does not affect the *C*-AFM-$P2_1/m$ phase.[13] Remarkable hysteresis in both $M(H)$ and $\rho(H)$ is observed at 80 K [Fig. 1(b)], but is absent for $M(H)$ at 5 K [see Fig. 2(a)] in compliance with the above conclusion.

Applied pressure strongly increases M_0 of $La_{0.1}Ca_{0.9}MnO_3$ [Figs. 2(a) and 2(b)] and decreases resistivity by about 35%, at $T=80$ K. The increasing of magnetoresistance under pressure correlates with the enhancement of the FM volume fraction [see Fig. 2(b)]. However, the volume fraction of *C*-AFM-$P2_1/m$ phase in $La_{0.1}Ca_{0.9}MnO_3$ at 20 K is of about 20%,[12] namely, even its full transformation to *G*-AFM+FM-*Pnma* phase is not adequate to explain more than twofold increase of FM-phase volume under a modest pressure of about 11 kbar. In principle, two scenarios may be responsible for the increase in M_0 with increasing pressure: (i) An increase of the volume of FM droplets, inside the *G* -AFM matrix, and (ii) an increase of the canting angle of the *G*-AFM moments. Taking into account that the concentration of magnetic droplets in *G*-AFM matrix is proportional to $1-x$, and that in $La_{0.09}Ca_{0.91}MnO_3$ (see Refs. 12,13) with similar values of La doping and magnetization, the total cluster contribution to the sample-average magnetization is only of about 10%, one may suppose that the increase in the canting angle is responsible for the increase of M_0 under pressure. At the same time, the pressure-induced enhancement of both conductivity and magnetoresistance in the magnetically ordered state [Fig. 3(a)] probably implies that the enhancement of the volume of FM droplets also gives rise to M_0 under pressure.

Let us discuss the magnetic and transport properties of $La_{0.2}Ca_{0.8}MnO_3$. The peak in magnetization at $T \sim 215$ K (Fig. 4) is associated with a structural phase transition from high temperature *Pnma* structure to $P2_1/m$ structure.[10–13] At temperatures below the magnetization maximum, the lattice parameter *b* undergoes a significant decrease while the *a* and *c* axes parameters slightly increase.[10] The structural phase transition is also associated with the polarization of $d_{3z^2-y^2}$ orbitals along the $(10\bar{1})$ direction, facilitating DE along the FM chains characteristic of *C*-AFM.[12] Despite the conclu-

sion of Pissas *et al.*[10] on the second-order structural phase transition involving continuous change of cation displacements, a pronounced hysteresis of the magnetization for the cooling and heating was observed, denoting a first-order transition. In compliance with previous investigations[10,11] no evidence was found for a FM moment in the monoclinic phase (see inset in Fig. 4). This observation agrees with the conclusion that all e_g electrons participating in FM double exchange along the $(10\bar{1})$ chain directions of *C*-AFM structure rather than forming FM clusters.[12] Applied pressure of 11.2 kbar (Fig. 4) slightly decreases the magnetization in the vicinity of the $M(T)$ peak and narrows the thermal hysteresis. The above observation showing a near insensitivity of T_{OO} to an applied pressure indicates the high robustness of the orbital ordered state in $La_{0.2}Ca_{0.8}MnO_3$. Recent investigation of the stability of the CO/OO state in $La_{1-x}Ca_xMnO_3$ ($0.5 < x < 0.9$) has shown that in contrast to $x=0.5,0.55$ cases, the CO/OO temperature for $x=0.75$ and 0.8 is independent of high magnetic fields up to $H<140$ kOe.[26] Combined data of resistivity, magnetization, ultrasound, and crystallography show that the strong increase of the Q_3 cooperative Jahn-Teller distortion mode occurs at the expense of Q_2, leading to concomitant suppression of FM and PS tendencies, and it is responsible for the robustness of charge/orbital ordered state at $x=0.75-0.8$.[26] Q_2 is an orthorhombic distortion, with the in-plane bonds differentiating into a long and a short one. Q_3 is the tetragonal distortion with the in-plane bond lengths shortening and out-of-plane bonds extending, or vice versa.[27,28]

Figure 5 shows that a variation of E_a in a single activation model is relatively small above 250 K. The temperature dependence of E_a shows that the simple activation form $\rho(T) = \rho_0 \exp(E_a/k_B T)$ may not be appropriate for the whole temperature range. At the same time, such a presentation may be very useful to follow the changes in the conduction mechanism.[24,29] As pointed out earlier, the E_a increase upon cooling from ~240 K is associated with the formation of OO, while the drop of the E_a at $T<185$ K is probably attributed to entering of AFM order. It should be noted that in recent ND studies[11,12] of $La_{0.2}Ca_{0.8}MnO_3$, it was realized that the temperatures of AFM ordering T_N and orbital ordering T_{OO} coincide. On the other hand, Pissas *et al.*[10] using ND data for $La_{0.2}Ca_{0.8}MnO_3$, have revealed that the monoclinic angle increases from 90° at ~205 K to ~91.5° at low temperatures, while the ordered Mn magnetic structure is observed only at a lower temperature of about 180 K. The study of electron magnetic resonance[30] (EMR) of our $La_{0.2}Ca_{0.8}MnO_3$ has shown the vanishing of EMR signal below 190 K, indicating the establishing of AFM ordering at $T_N < T_{OO}$. It appears that the broad magnetization peak (at ~210 K) may be attributed to the hopping of the e_g electrons at $T>T_{OO}$, which brings about FM correlations through the DE mechanism. At a decreasing temperature these electrons freeze and the FM fluctuations are replaced by a superexchange-driven AFM spin configuration.[10] The reduction of magnetization under pressure at $T>T_{OO}$ implies that the partial suppression of FM fluctuations may in turn promote AFM ones and may lead to hysteresis narrowing.

The combined magnetization and ND measurements[10–13] for electron-doped LCMO have shown that the sample with $x=0.8$ undergoes an orthorhombic-to-monoclinic structural transition (at $T\sim200$ K), concurrent with a transition to AFM state and *C*-type magnetic structure. At low temperatures, the monoclinic fraction approaches about 80% of the volume. In addition, the sample with $x=0.9$ exhibits one structural and two magnetic transitions T_N(*C*-AFM) and T_N(*G*-AFM), that results in mesoscopic phase separation of *C*-AFM regions with no FM component and regions where the long-range FM component is perpendicularly coupled to the *G*-AFM structure.[12] The high enough density of FM clusters results in a formation of a FM spin cluster glass,[12] manifested by the significant difference between FC and ZFC curves (see Fig. 1). Our magnetic and transport measurements at ambient pressure are essentially consistent with the ND results. There are some disagreements between our results and those observed by Ling *et al.*[12] In conclusion, magnetic measurements and structural data show that the characteristics features observed in our samples are similar to those of Pissas group.[10,11] The difference in the results of Ling *et al.*[12] and our observation may be attributed to the difference in the sample preparation.

Recent investigations of hole-doped manganites at higher pressures (>20 kbar)[24,29,31–34] have shown that at relatively low pressures (~10–15 kbar), $dT_C/dP>0$, but may progressively decrease at higher pressure.[29,31,33] Postorino *et al.*[31] have pointed out that the AFM interaction increases sufficiently at higher pressures ($P>40$ kbar). This may lead to the compensation of the effect of pressure on T_C. The dominant effect on dT_C/dP at relatively low pressures (<20 kbar) stems from a pressure-induced increase of the hopping integral and weakening of electron-phonon coupling. In this regard, a further study of structural, transport, and magnetic properties as well as changes in orbital ordering temperature of electron-doped LCMO at higher pressures may provide new information on the mechanism of charge localization and balance of competing interactions.

In conclusion, we have found that FM component in the *G*-AFM fraction of $La_{0.1}Ca_{0.9}MnO_3$ is very sensitive to modest applied pressure. A pressure of 11 kbar doubles the spontaneous magnetization. Remarkable hysteretic effects observed in both $M(H)$ and $\rho(H)$ dependences of $La_{0.1}Ca_{0.9}MnO_3$ below magnetic ordering temperature manifest significant competition of FM and AFM components in *G*-type AFM structure. In the case of $La_{0.2}Ca_{0.8}MnO_3$, an applied pressure slightly narrows the range of thermal hysteresis associated with orbital ordering, whereas AFM ordering is practically insensitive to pressure. The variation of an activation energy of $La_{0.2}Ca_{0.8}MnO_3$ with temperature indicates a process of successive transitions to an orbital ordered state at ~210 K, and then to an AFM state with no FM component at ~185 K.

This research was supported by the Israeli Science Foundation administered by the Israel Academy of Sciences and Humanities (Grant No. 209/01).

*Electronic address: markoviv@bgumail.bgu.ac.il

[1] E. Dagotto, *Nanoscale Phase Separation and Colossal Magnetoresistance*, Springer Series in Solid State Physics (Springer-Verlag, Berlin, 2003).
[2] J. B. Goodenough, *Rare Earth-Manganese Perovskites*, Handbook on the Physics and Chemistry of Rare Earth Vol. 33, edited by K. A. Gschneidner Jr., J.-C. G. Bunzli, and V. K. Pecharsky (Elsevier Science, Amsterdam, 2003).
[3] E. O. Wollan and W. C. Koehler, Phys. Rev. **100**, 545 (1955).
[4] J. B. MacChesney, H. J. Williams, J. F. Potter, and R. C. Sherwood, Phys. Rev. **164**, 779 (1967).
[5] J. J. Neumeier and J. L. Cohn, Phys. Rev. B **61**, 14 319 (2000).
[6] H. Fujishiro, M. Ikebe, S. Ohshiden, and K. Noto, J. Phys. Soc. Jpn. **69**, 1865 (2000).
[7] C. Martin, A. Maignan, M. Hervieu, B. Raveau, Z. Jirak, M. M. Savosta, A. Kurbakov, V. Trounov, G. Andre, and F. Bouree, Phys. Rev. B **62**, 6442 (2000).
[8] L. Sudheendra, A. R. Raju, and C. N. R. Rao, J. Phys.: Condens. Matter **15**, 895 (2003).
[9] C. Martin, A. Maignan, M. Hervieu, and B. Raveau, Phys. Rev. B **60**, 12 191 (1999).
[10] M. Pissas, G. Kallias, M. Hofmann, and D. M. Többens, Phys. Rev. B **65**, 064413 (2002).
[11] M. Pissas and G. Kallias, Phys. Rev. B **68**, 134414 (2003).
[12] C. D. Ling, E. Granado, J. J. Neumeier, J. W. Lynn, and D. N. Argyriou, Phys. Rev. B **68**, 134439 (2003).
[13] E. Granado, C. D. Ling, J. J. Neumeier, J. W. Lynn, and D. N. Argyriou, Phys. Rev. B **68**, 134440 (2003).
[14] J. J. Neumeier, M. F. Hundley, J. D. Thompson, and R. H. Heffner, Phys. Rev. B **52**, R7006 (1995).
[15] H. Y. Hwang, T. T. M. Palstra, S.-W. Cheong, and B. Batlogg, Phys. Rev. B **52**, 15046 (1995).
[16] J. M. De Teresa, M. R. Ibarra, J. Blasco, J. Garcia, C. Marquina, P. A. Algarabel, Z. Arnold, K. Kamenev, C. Ritter, and R. von Helmolt, Phys. Rev. B **54**, 1187 (1996).
[17] T. Okuda, Y. Tomioka, A. Asamitsu, and Y. Tokura, Phys. Rev. B **61**, 8009 (2000).
[18] V. Markovich, I. Fita, R. Puzniak, M. I. Tsindlekht, A. Wisniewski, and G. Gorodetsky, Phys. Rev. B **66**, 094409 (2002).
[19] V. Markovich, I. Fita, R. Puzniak, E. Rozenberg, A. Wisniewski, C. Martin, A. Maignan, M. Hervieu, B. Raveau, and G. Gorodetsky, Phys. Rev. B **65**, 224415 (2002).
[20] G. Garbarino, C. Acha, D. Vega, G. Leyva, G. Polla, C. Martin, A. Maignan, and B. Raveau, Phys. Rev. B **70**, 014414 (2004).
[21] V. Markovich, I. Fita, R. Puzniak, E. Rozenberg, C. Martin, A. Wisniewski, A. Maignan, B. Raveau, Y. Yuzhelevski, and G. Gorodetsky, Phys. Rev. B **70**, 024403 (2004).
[22] D. L. Huber, G. Alejandro, A. Caneiro, M. T. Causa, F. Prado, M. Towar, and S. B. Oseroff, Phys. Rev. B **60**, 12 155 (1999).
[23] T. Penney, M. W. Shater, and J. B. Torrance, Phys. Rev. B **5**, 3669 (1972).
[24] C. Cui and T. A. Tyson, Appl. Phys. Lett. **83**, 2856 (2003).
[25] P. A. Algarabel *et al.*, Phys. Rev. B **65**, 104437 (2002).
[26] X. G. Li, R. K. Zheng, G. Li, H. D. Zhou, R. X. Huang, J. Q. Xie, and Z. D. Wang, Europhys. Lett. **60**, 670 (2002); R. K. Zheng, G. Li, A. N. Tang, Y. Yang, W. Wang, X. G. Li, Z. D. Wang, and H. C. Ku, Appl. Phys. Lett. **83**, 5250 (2003).
[27] Y. Yamada, O. Hino, S. Nohdo, R. Kanao, T. Inami, and S. Katano, Phys. Rev. Lett. **77**, 904 (1996).
[28] B. B. Van Aken, A. Meetsma, Y. Tomioka, Y. Tokura, and T. T. M. Palstra, Phys. Rev. B **66**, 224414 (2002).
[29] C. Cui and T. A. Tyson, Phys. Rev. B **70**, 094409 (2004).
[30] A. I. Shames, E. Rozenberg, M. Auslender, G. Gorodetsky, C. Martin, A. Maignan, and Ya. M. Mukovskii, J. Magn. Magn. Mater. **290–291**, 910 (2005).
[31] P. Postorino, A. Sacchetti, M. Capone, and P. Dore, Phys. Status Solidi B **241**, 3381 (2004).
[32] C. Meneghini, D. Levy, S. Mobilio, M. Ortolani, M. Nunez-Reguero, A. Kumar, and D. D. Sarma, Phys. Rev. B **65**, 012111 (2001).
[33] A. Congeduti, P. Postorino, E. Caramagno, M. Nardone, A. Kumar, and D. D. Sarma, Phys. Rev. Lett. **86**, 1251 (2001); P. Postorino, A. Congeduti, P. Dore, A. Sacchetti, F. Gorelli, L. Ulivi, A. Kumar, and D. D. Sarma, *ibid.* **91**, 175501 (2003).
[34] D. P. Kozlenko, V. P. Glazkov, R. A. Sadykov, B. N. Savenko, V. I. Voronin, and I. V. Medvedeva, J. Magn. Magn. Mater. **258–259**, 290 (2003).